Acta Cryst. (1980). A**36**, 183–189

Phase-Angle Determination by Anomalous X-ray Scattering with a Four-Circle SSD Diffractometer

BY T. SAKAMAKI AND S. HOSOYA

Institute for Solid State Physics, University of Tokyo, 7-22-1 *Roppongi, Minato-ku, Tokyo* 106, *Japan*

AND T. FUKAMACHI

Saitama Institute of Technology, Fusaiji, Okabe, Saitama 369-02, *Japan*

(*Received* 14 *August* 1979; *accepted* 25 *September* 1979)

Abstract

By the use of a four-circle diffractometer with a solid-state detector, the integrated Bragg reflexion intensities from hemimorphite [$Zn_4Si_2O_7(OH)_2.H_2O$] have been measured by energy-dispersive diffractometry at three energy values, including the region very near the Zn *K* absorption edge. The anomalous difference Patterson map obtained indicated Zn–Zn peaks. By the use of the anomalous-scattering effect to the maximum extent, the phases of one hundred reflexions have been determined with a mean error of 15·4°.

Introduction

Anomalous or resonance scattering has been used in structure analyses in various ways. In the case of neutron diffraction, several attempts have been reported (*e.g.* Dale & Willis, 1966; Koetzle & Hamilton, 1975; Sikka & Rajagopal, 1975): the usual neutron beam from reactors normally has a white spectrum from which a narrow energy band is selected by a monochromator. Its relevant anomalous or resonance scattering is relatively large. Recently a more effective application of neutron anomalous scattering to phase-angle determination has been published by Bartunik (1978). However, the number of isotopes which cause the anomalous scattering effect at suitable energy values is more or less limited both in species and natural abundance, and it is often necessary to carry out isotope condensation in the specimen.

Nuclear resonance scattering is three orders of magnitude larger than X-ray anomalous scattering, but there are several demerits; the available convenient nuclear species are rather limited, the brilliancy of the radioactive source cannot be made higher because of its self-absorption, and isotope condensation in samples is difficult when the relevant isotope has a short life. Various efforts, however, have been made to overcome these difficulties (Mössbauer, 1973, 1975). Recently, Cohen, Miller & West (1978) have reported their success in selecting the very narrow energy band corresponding to the nuclear resonance γ-ray from synchrotron radiation by a suitable narrow time window. There have been at least two other attempts in this field (Artemyev, Kabannik, Kazakov, Kulipanov, Meleshko, Sklyarevskiy, Skrinsky, Stepanov, Khlestov & Chechin, 1978; Kagan, Afanas'ev & Kohn, 1979). This might suggest the possibility of the feasible future use of nuclear resonance scattering.

On the other hand, X-ray anomalous scattering can be observed from various atoms over a fairly wide range. Many years ago, it was pointed out that white radiation may be used for this purpose by changing the diffraction angle for each Laue spot (Grenville-Wells & Lonsdale, 1954). A recent example is the use of two characteristic X-rays for determining the phases of erythrocruorin (Hoppe & Jakubowski, 1975). Then, by the best use of an SSD (solid-state detector), it was shown that the determination of the anomalous-scattering factors as functions of energy and some applications of these factors such as polarity determination are feasible in a typical laboratory (Hosoya & Fukamachi, 1973; Hosoya, 1975; Fukamachi & Hosoya, 1975; Fukamachi, Hosoya & Okunuki, 1976*a*,*b*; Fukamachi, Hosoya, Kawamura & Okunuki, 1977, 1979). Concurrently, the advent of synchrotron radiation has opened great possibilities in this field (Bonse & Materlik, 1976; Phillips, Wlodawer, Yevitz & Hodgson, 1976; Hodgson, Phillips & Wlodawer, 1976; Phillips, Wlodawer, Goodfellow, Watenpaugh, Sieker, Jensen & Hodgson, 1977; Fukamachi, Hosoya, Kawamura & Hastings, 1977; Fukamachi, Hosoya, Kawamura, Hunter & Nakano, 1978).

The present paper describes consecutive procedures for determining the anomalous-scattering curves, for measuring intensities and for determining phase angles by the use of a four-circle SSD automatic diffractometer. The features of this apparatus will be reported elsewhere.

0567-7394/80/020183-07$01.00

Determination of the $f'(E)$ and $f''(E)$ values

As a test case, a known structure, hemimorphite (Table 1), has been chosen because it contains eight Zn atoms in a cell and the structure is noncentrosymmetric (Ito & West, 1932; Barclay & Cox, 1960; McDonald & Cruickshank, 1967; Hill, Gibbs, Craig, Ross & Williams, 1977). It is expected that the anomalous-dispersion effects will occur to a sufficient degree. In order to determine the phase angle by the use of anomalous scattering, it is necessary to determine the values of f' and f'' as a function of energy E. In order to carry this out, the method previously reported (Fukamachi, Hosoya, Kawamura & Okunuki, 1977) was used: the $f''(E)$ curve was determined at about 1400 eV by absorption measurement on a sample plate about 34 μm thick, using an SSD diffractometer, with a Si monochromator and a Cu tube operated at 30 kV and 38 mA. This took about 3 days and then the $f'(E)$ curve was calculated by the use of the dispersion relation, as shown in Fig. 1. In the present set-up, the energy resolution is estimated to be about 4 eV, being limited solely by the slit system because the lattice constants of the specimen crystal show no appreciable variation (Fukamachi, Hosoya & Terasaki, 1973; Hosoya, 1975; Buras, Niimura & Olsen, 1978).

The broken lines in Fig. 1 show the values calculated by the use of the formula proposed by Parratt & Hempstead (1954) with the values of the oscillator strength obtained by Cromer (1965). The formula of Parratt & Hempstead was derived with a free-atom approximation, and therefore the formula naturally cannot explain the fine structures on the high-energy side of the absorption edge. Apart from that, however, the theoretical curves agree fairly well with the experimental values.

Table 1. *Crystal data of hemimorphite*

$Zn_4Si_2O_7(OH)_2.H_2O$
$Z = 2$
Space group *Imm*2
$a = 8{\cdot}37$, $b = 10{\cdot}72$, $c = 5{\cdot}12$ Å

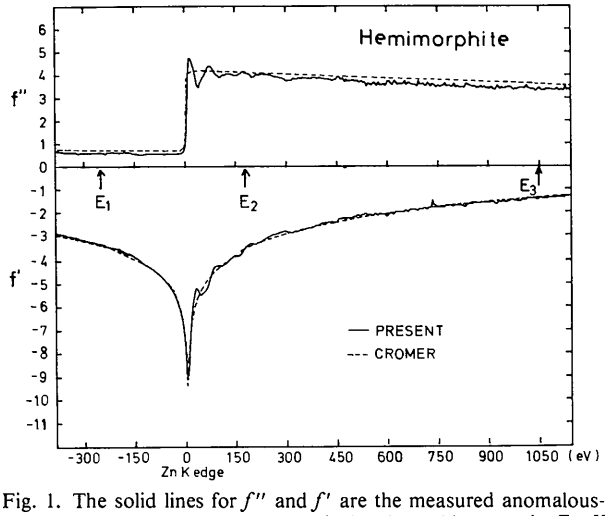

Fig. 1. The solid lines for f'' and f' are the measured anomalous-scattering factors for a Zn atom in hemimorphite near the Zn K absorption edge (9·66 keV). Broken lines were calculated by the formula of Parratt & Hempstead.

Fig. 2 shows the dependence of the energy profiles of Bragg reflexions upon the Bragg angle. These are obtained by numerical integration in the case of kinematical diffraction. Fig. 2 indicates, for instance, that the measured X-rays are about 400 eV in energy breadth at $E_0 = 9{\cdot}66$ keV and at the Bragg angle $\theta = 10°$. Therefore, the values derived from the Parratt & Hempstead formula are good enough to be used in energy-dispersive diffractometry.

Integrated intensity measurements by energy-dispersive diffractometry

The measurements were carried out on the integrated intensity from a hemimorphite spherical sample ground to a radius of 0·14 mm. In the energy-dispersive method, the integrated intensity of each reflexion is measured with both the detector and the crystal fixed, this being different from the angle-dispersive method. The X-ray tube with a Cu target was operated at 30 keV and 20 mA. Each reflexion was measured for 35 min, but for stronger reflexions measurement was stopped when the number of counts reached ten thousand. In order to eliminate the fluorescence X-rays, background counts were measured on both sides $\pm 2°$ away from the Bragg condition around the ω axis, and were then subtracted. Almost all (about 149) reflexions

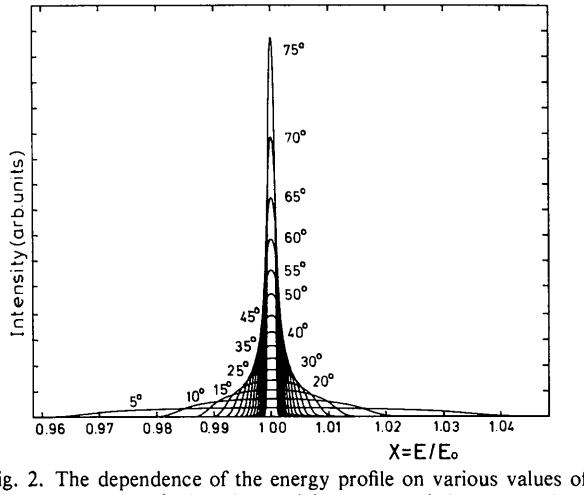

Fig. 2. The dependence of the energy profile on various values of the Bragg angle θ when the receiving aperture is large enough to receive the white X-rays. These were obtained by numerical integration for the system used, where the distance from the entrance aperture to the crystal is 375 mm, the inner diameter of the collimator is 0·5 mm and the sample is a spherical mosaic crystal 0·28 mm in diameter.

with an interplanar spacing greater than 1 Å were measured. The integrated intensities were measured at three energy values indicated by arrows in Fig. 1. Experimental conditions are summarized in Table 2. The white X-rays are two orders of magnitude weaker per energy width than the characteristic X-rays, but owing to the use of energy-dispersive diffractometry, the measurement time is not as long as expected (see Table 2). The X-rays used in the present set-up were checked by a crystal with a known structure, and proved to be practically unpolarized in accord with the results of Staun Olsen, Buras, Jensen, Alstrup, Gerward & Selsmark (1978).

Table 2. *Experimental conditions*

	E_1	E_2	E_3
Energy (keV)	9·406	9·840	10·710
Data-collecting time (days)	4	8	7
Number of reflexions	149 × 2	149 × 2	155 × 2
f'	−3·38	−3·38	−1·38
f''	0·61	4·10	3·36
μ (mm^{-1})	12	52	48

Derivation of the structure factors

According to the kinematical theory, the integrated intensity measured with unpolarized X-rays, on a relative basis, by the energy-dispersive method is given by the following expression:

$$J_h(E) \propto I_o(E) A_h(\theta)[(1 + \cos^2 2\theta)|F_h|^2/(E^2 \sin^2 \theta)], \quad (1)$$

where the incident continuous X-rays, $I_o(E)$, are assumed to be smooth in the energy intensity distribution, $A_h(\theta)$ is the absorption factor, E the energy of the relevant X-rays, F_h the structure factor and θ the Bragg angle. However, X-rays from an ordinary sealed-off tube do not have a smooth energy intensity distribution. In particular, in the energy region very near the Zn K absorption edge (9·66 keV), the WL spectrum appears, this being due to the tungsten layer on the anode evaporated from a filament. In Fig. 3 the relative intensities of several WL lines are shown on a logarithmic scale. This spectrum was obtained by analysis with the 444 reflexion from a Si 111 monochromator. Namely, the incident X-ray intensity, $I_0(E)$, at each Bragg angle was estimated according to the dynamical theory in the Bragg case, assuming that Si is a perfect crystal. Moreover, in energy-dispersive diffractometry, the energy resolution varies with the diffraction angle 2θ. Therefore, the relative values of the $|F_h|$'s are calculated not by equation (1) but by the following approximate expression:

$$\begin{aligned} J_h \propto \sum_i W(E_i, \theta_i) I_0(E_i) A_h(E_i) \Big| \sum_j \{f_j + f'_j(E_i) \\ + if''_j(E_i)\} \\ \times \exp(2\pi i \mathbf{h}\mathbf{x}_j)\Big|^2 [(1 + \cos^2 2\theta_i)/(E_i^2 \sin^2 \theta_i)] \\ \simeq A_h(E_B)|F_h(E_B)|^2 \left\{\left[\sum_i W(E_i, \theta_B) I_0(E_i)\right]\right. \\ \left. \times (1 + \cos^2 2\theta_B)/(E_B^2 \sin^2 \theta_B)\right\}, \end{aligned} \quad (2)$$

where $W(E_i, \theta_B)$ is the ratio of X-rays with energy E_i (diffracted at each Bragg angle θ_B shown in Fig. 2), and $I_0(E_i)$ the intensity distribution shown in Fig. 3. The summation over i is taken for all energy values of X-rays diffracted at each Bragg angle θ_B. In this case, the correction factor in square brackets in expression (2) was 4% at maximum.

Among the 149 independent reflexions measured, 100 reflexions were used in the following data analyses: 41 reflexions had intensities smaller than $3\sigma(F)$, where the standard deviation $\sigma(F)$ was estimated from counting statistics, and 8 reflexions in a lower-angle region extended over the Zn K absorption edge because of their low energy resolution.

Two-energy anomalous difference Patterson map

If there are anomalously scattering atoms of only one type in the unit cell, then

$$I_1 = (|F_1|^2 + |\bar{F}_1|^2) = |F_N|^2 + (f_1'^2 + f_1''^2)|\chi|^2 + 2|F_N||f_1||\chi| \cos \varphi$$

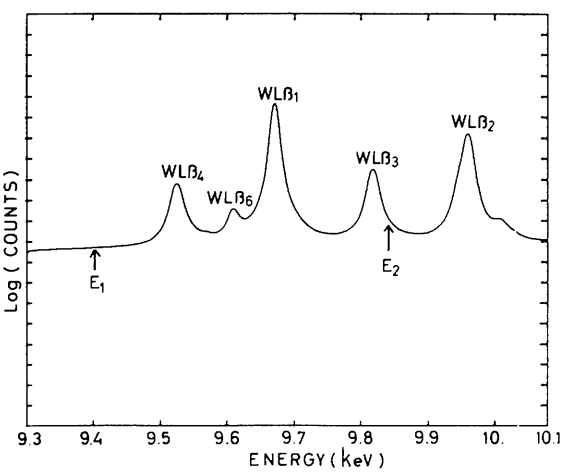

Fig. 3. An incident X-ray spectrum near the Zn K absorption edge.

and

$$I_2 = (|F_2|^2 + |\bar{F}_2|^2) = |F_N|^2 + (f_2'^2 + f_2''^2)|\chi|^2 + 2|F_N| f_2 |\chi| \cos\varphi,$$

where subscripts 1 and 2 refer to the two energy values; $|F_N|$ is the structure factor due to those atoms which do not scatter anomalously; f is $f_0 + f'(E)$; $|\chi|$ is the geometric structure factor of anomalously scattering atoms and φ is the angle between the f vector and the $|F_N|$ vector in the Argand diagram. If $f_1 = f_2$, then

$$I_2 - I_1 = (f_2'' - f_1'')|\chi|^2.$$

Therefore, an anomalous difference Patterson map computed with $I_2 - I_1$ as coefficients contains the interatomic peaks among anomalous scatterers only, as was pointed out by Sikka (1969) in the neutron case. In principle, this difference Patterson map should be simple, if it includes relatively little noise, because the relevant atoms are all equal in weight. Therefore, the systematic method for unravelling the periodic vector set (Tokonami & Hosoya, 1965) may be applied more easily than in the usual Patterson map. Moreover, the mathematical procedures proposed by Goldak (1969, 1971, 1974) for obtaining the periodic vector set from the anomalous difference Patterson map may work better, if they work at all.

In the present work, the X-ray anomalous difference Patterson map was calculated for the first time by the use of data sets measured at E_1 and E_2 (Fig. 4). The relative scale was determined by the condition: $\sum (|F_1| + |\bar{F}_1|) = \sum (|F_2| + |\bar{F}_2|)$. The data scaled in this way did not give a reasonable anomalous difference Patterson map: the Patterson function was negative in the position where a Zn–Zn peak should appear. This may come from the difficulty of finding the correct scale factor between the two sets of data. The anomalous Patterson maps were calculated by changing the scale factor by a step of 2%, starting from the scale giving the total summation of $|F|$ equal at the two energies. Fig. 4(*b*) shows the anomalous difference Patterson map calculated by scaling such that the data measured at the energy E_2 were multiplied by 1·10. For comparison, in Fig. 4(*a*) is shown the ordinary Patterson map calculated with the data measured at energy E_2. The Zn–Zn peaks are shown by cross marks in Fig. 4, but other peaks also appear in the anomalous difference Patterson map. This map proved to be sensitively influenced by the accuracy of the measurements.

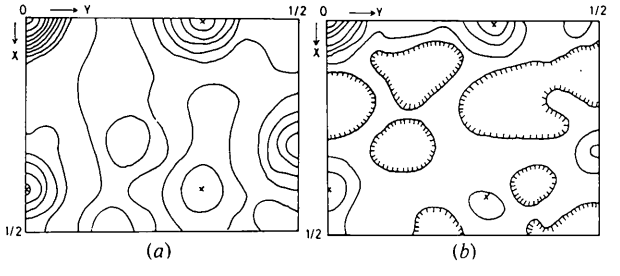

(*a*) (*b*)

Fig. 4. (*a*) Ordinary Patterson map and (*b*) anomalous difference Patterson map. Both show Harker sections at $z = 0$.

Phase determination

The atomic coordinates of a Zn atom determined from the anomalous difference Patterson map, together with the temperature factor of the Zn atoms and the scale factor obtained by a Wilson plot were refined by the block-diagonal least-squares method by the use of each energy data set. The scale factors obtained by this method are larger than the true values, because only Zn atoms are taken into account in the least-squares refinement. For the coordinates and temperature factors of Zn atoms, the average values obtained by this method were used in the following analysis.

Subsequently, both the refinement of the Zn atomic parameters and the determination of the phases were carried out simultaneously: the determination of the phases by the use of anomalous scattering was carried out in the same way as described by Herzenberg & Lau (1967). Fig. 5 shows the phase determination of the 431 reflexion as an example: the curve labelled as E_1, E_2 and E_3 shows the energy dependence of the anomalous scattering contributing to this reflexion, while the curve labelled as E_1^*, E_2^* and E_3^* shows a corresponding curve for the $\bar{4}31$ reflexion.

The measurements were carried out at three energy values, so that six circles corresponding to three Friedel pairs are available. In principle, the six circles must intersect at one point, but because of the experimental errors and the inaccuracy in the absolute scale factor, the circles do not exactly intersect at one point.

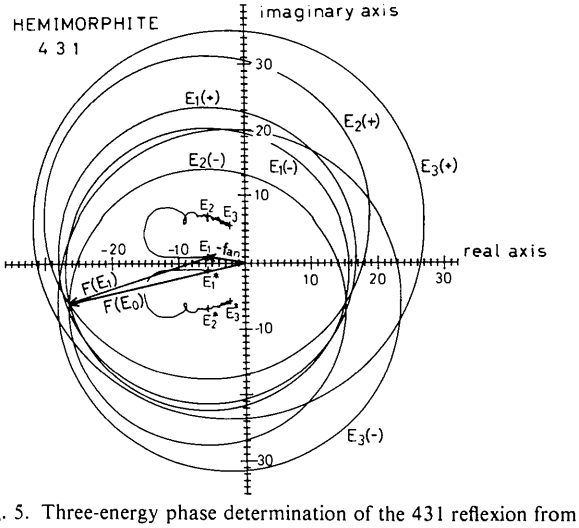

Fig. 5. Three-energy phase determination of the 431 reflexion from hemimorphite. The details are given in the text.

Therefore, the probability of each phase has been calculated in the same way as described by Blow & Crick (1959) by the use of the probability function,

$$P(\varphi) = \prod_{j=2}^{n} \exp\{-[X_j(\varphi) - \bar{X}]^2/2\langle\sigma_j\rangle\}, \qquad (3)$$

where $\langle\sigma_j\rangle$ is the standard deviation of the closure errors and $X_j(\varphi) - \bar{X}$ is the lack of closure for the phase triangle. There is practically no energy region free from anomalous dispersion, so that the structure factors of the plus reflexions of the Friedel pair measured at E_1 were used as $\bar{X}$. In the present case, the probability distribution was computed by the use of the data set measured at three energies (Fig. 6). The value to be minimized is

$$\sum_j \sum_h [|F_h(E_j)| - |D_h(E_j)|]^2,$$

where $|F_h(E_j)|$ is the observed value, and

$$|D_h(E_j)| = K(E_j)[\{A'_h(E_j) + |F_h(E_1)| \cos\varphi_h\}^2 + \{B'_h(E_j) + |F_h(E_1)| \sin\varphi_h\}^2]^{1/2},$$

where φ_h is the best phase obtained by the use of equation (3), $K(E_j)$ is the scale factor for the data measured at each energy, and $A'_h(E_j)$ and $B'_h(E_j)$ are given by

$$A'_h(E_j) = A_h(E_j) - A_h(E_1)$$

and

$$B'_h(E_j) = B_h(E_j) - B_h(E_1),$$

where $A_h(E_j)$ and $B_h(E_j)$ are the structure factor terms arising from anomalous-scattering effects only. If the temperature factor is ignored, the following formula is obtained:

$$A_h(E_j) + iB_h(E_j) = \sum \{f'_k(E_j) + if''_k(E_j)\} \times \exp\{2\pi i(\mathbf{hx}_k)\}.$$

The atomic parameters of Zn and the scale factors were refined until the change of the mean phase angle was reduced to less than 5°. Table 3 shows the final atomic parameters. Table 4 shows the final best phases φ_b obtained, together with the phases φ_c calculated by the use of the atomic parameters determined by Takéuchi, Sasaki, Joswig & Fuess (1978). The mean phase error from φ_c is as small as 15·4°, because three redundant data sets measured at three different energies were used, and also because the anomalous-scattering effect sufficiently contributed to the structure factor owing to the small unit cell of the crystal.

The intensity-ratio method (Hosoya, 1975) should be, in principle, less subject to errors: it is not necessary to determine the absolute intensity, and if the sample has a suitable symmetry in shape then it is not necessary to know the absorption coefficient because it often does not affect the Friedel-pair intensity ratio (Cole & Stemple, 1962; Holloway, 1969; Fukamachi, Hosoya & Okunuki, 1976*b*). However, in practice, the intensity ratio is often near unity and the ratio circles become large, the crossing points scatter (at least apparently), and it is difficult to determine the real solution point. Thus small errors in the ratio value may cause a large deviation from the real solution point, even if the phase-angle value itself does not necessarily change much.

Discussion and conclusion

By the use of white X-rays, the X-ray anomalous difference Patterson synthesis was carried out for the first time. It was found that high accuracy of the measurements is required for this purpose. As for the phase determination, after the coordinates of anomalous atoms were found, the required accuracy in the intensity measurements is not so high as in the Patterson synthesis. Even if the structure factors measured have relatively large errors, the relevant inter-

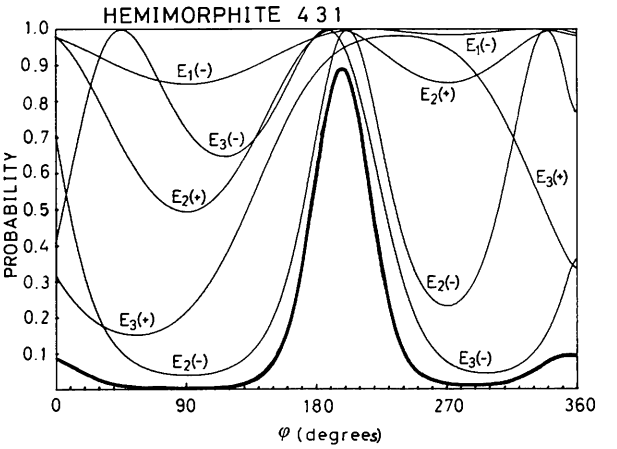

Fig. 6. Joint probability for phase distribution (thick solid line) for the 431 reflexion from hemimorphite. Each curve labelled as $E_i(\pm)$ shows the relevant probability distribution for the structure factor measured at each energy i to make a phase triangle for a plus reflexion measured at energy E_1.

Table 3. *Atomic parameters of* Zn

	Takéuchi *et al.* (1978)	Present work
x	0·2045	0·2021
y	0·1612	0·1606
z	0·0	0·0
B_{11}	0·00248	0·00148
B_{22}	0·00162	0·00045
B_{33}	0·00561	0·00977
B_{12}	−0·00050	0·00347
B_{13}	−0·00005	0·00347
B_{23}	−0·00001	0·00028

Table 4. *Structure factors observed at three energies, phases φ_c calculated from the atomic parameters determined by Takéuchi et al. (1978), the best phases φ_b determined in the present work and their differences, $\Delta\varphi$*

			E_1		E_2		E_3				
h	k	l	$F(+)$	$F(-)$	$F(+)$	$F(-)$	$F(+)$	$F(-)$	φ_c	φ_b	$\Delta\varphi$
4	0	0	46.43	46.43	42.58	42.58	47.57	47.57	1.5	0.0	1.5
6	0	0	32.79	32.79	35.64	35.64	40.03	40.03	1.0	0.0	1.0
5	1	0	29.86	29.86	33.00	33.00	39.40	39.40	2.0	0.0	2.0
6	2	0	11.78	11.78	10.70	10.70	11.77	11.77	-178.7	13.5	167.8
3	3	0	45.32	45.32	45.86	45.86	52.51	52.51	1.3	0.0	1.3
5	3	0	72.02	72.02	66.08	66.08	76.37	76.37	-178.3	180.0	1.7
7	3	0	17.62	17.62	18.77	18.77	25.86	25.86	3.6	0.0	3.6
2	4	0	14.07	14.07	15.51	15.51	19.90	19.90	2.6	0.0	2.6
1	5	0	15.76	15.76	15.81	15.81	17.71	17.71	0.5	0.0	0.5
3	5	0	18.28	18.28	19.02	19.02	21.80	21.80	-178.3	180.0	1.7
5	5	0	15.48	15.48	16.18	16.18	19.81	19.81	2.1	0.0	2.1
0	6	0	82.83	82.83	79.02	79.02	89.40	89.40	1.5	0.0	1.5
2	6	0	26.46	26.46	30.34	30.34	37.28	37.28	-177.6	180.0	2.4
4	6	0	31.06	31.06	33.66	33.66	39.99	39.99	1.7	0.0	1.7
6	6	0	19.48	19.48	19.31	19.31	22.71	22.71	1.5	0.0	1.5
1	7	0	18.73	18.73	19.23	19.23	22.59	22.59	2.3	0.0	2.3
3	7	0	6.14	6.14	9.60	9.60	5.74	5.74	-5.5	0.0	5.5
5	7	0	29.11	29.11	31.13	31.13	38.24	38.24	2.7	0.0	2.7
2	8	0	13.84	13.84	13.02	13.02	16.06	16.06	2.3	0.0	2.3
1	9	0	15.84	15.84	15.10	15.10	19.28	19.28	-177.6	180.0	2.4
3	9	0	17.97	17.97	19.40	19.40	25.20	25.20	3.3	0.0	3.3
0	10	0	23.23	23.23	26.04	26.04	32.64	32.64	-176.2	180.0	3.8
3	0	1	47.58	41.13	41.77	47.23	49.16	53.95	156.6	174.0	17.4
5	0	1	27.75	24.41	31.51	30.38	40.45	39.83	2.2	4.5	2.3
7	0	1	36.34	31.83	41.06	38.54	51.18	48.71	-176.2	-177.0	0.8
4	1	1	4.06	3.57	6.33	2.55	5.74	2.88	48.2	97.0	48.8
3	2	1	23.60	22.47	22.88	27.72	28.39	31.99	-32.0	-49.0	17.0
5	2	1	21.47	20.84	22.62	22.45	28.24	27.23	-170.6	174.0	15.4
7	2	1	19.58	18.88	19.20	18.73	24.22	24.94	6.8	-5.5	12.3
2	3	1	51.20	48.25	44.83	51.23	55.34	59.14	-16.0	-5.5	10.5
4	3	1	22.36	21.29	24.14	20.57	29.39	25.81	-149.0	-154.5	5.5
1	4	1	11.77	11.72	11.99	9.85	14.13	11.57	-120.5	-100.5	20.0
3	4	1	37.56	35.63	43.46	42.21	50.16	50.49	3.6	-15.0	18.6
5	4	1	22.66	21.76	23.84	21.69	30.46	29.33	-167.3	-170.5	3.2
7	4	1	23.88	11.62	23.59	25.91	30.21	32.47	-4.1	-6.5	2.4
0	5	1	17.09	17.51	16.66	19.89	19.84	23.39	-24.6	-50.0	25.4
2	5	1	19.61	19.64	18.63	19.96	23.12	24.44	169.4	146.0	23.4
4	5	1	12.34	12.01	11.06	9.94	13.55	12.70	33.3	78.5	45.2
1	6	1	4.85	4.38	7.40	5.73	8.28	5.47	39.4	58.5	19.1
3	6	1	33.62	33.47	35.49	39.09	43.93	47.54	175.1	164.5	10.6
5	6	1	24.18	23.45	25.66	25.65	34.35	34.50	4.6	5.5	0.9
0	7	1	28.78	28.36	34.18	28.24	39.17	36.90	18.0	11.5	6.5
2	7	1	38.43	38.84	45.50	44.37	51.91	52.45	-173.8	166.5	19.7
1	8	1	10.88	10.65	10.05	9.69	12.35	11.56	-168.5	-124.0	44.5
5	8	1	15.40	15.10	15.01	13.34	18.15	18.90	-170.7	-164.5	6.2
0	9	1	29.74	30.50	36.08	31.53	43.16	41.64	-166.5	-174.0	7.5
2	9	1	25.83	25.85	26.56	28.64	33.60	37.24	-4.4	-7.0	2.6
0	0	2	92.92	90.09	95.97	86.88	97.36	90.43	23.1	45.0	21.9
2	0	2	35.47	32.16	45.69	47.84	52.99	53.58	179.3	165.5	13.8
4	0	2	31.75	28.70	35.14	36.33	41.20	40.85	4.6	-20.0	24.6
6	0	2	20.63	18.15	20.59	19.87	24.25	22.39	43.7	34.5	9.2
1	1	2	13.70	12.72	15.13	12.90	17.06	14.65	37.4	58.5	21.1
3	1	2	13.92	13.00	12.72	15.46	17.54	19.74	164.6	150.0	14.6
5	1	2	23.13	20.42	24.07	24.10	30.91	29.26	9.3	0.5	8.8
0	2	2	16.34	16.18	21.12	16.39	24.28	20.66	-146.7	-163.0	16.3
2	2	2	20.57	19.24	22.99	20.04	27.16	25.04	12.4	13.0	0.6
4	2	2	10.53	10.10	8.05	11.08	10.60	13.15	135.0	106.5	28.5
1	3	2	26.52	25.21	30.50	27.32	34.78	31.49	-156.9	-174.0	17.1
3	3	2	32.07	29.22	37.65	33.09	45.32	40.82	14.8	8.5	6.3
5	3	2	53.14	47.65	50.63	47.32	60.38	58.32	-170.3	-161.5	8.8
7	3	2	22.70	20.98	22.33	25.46	31.39	32.61	-6.9	-3.0	3.9
0	4	2	31.52	31.45	35.09	38.14	42.14	45.47	167.4	160.5	6.9
2	4	2	18.70	18.44	18.02	20.19	24.01	25.32	-9.9	-10.5	0.6
4	4	2	16.80	16.38	16.47	15.09	20.38	19.72	-169.0	-156.5	12.5
1	5	2	10.05	10.50	10.55	8.59	10.64	9.69	98.4	88.5	9.9
3	5	2	12.62	12.18	13.73	11.01	16.08	14.31	-156.1	-129.5	26.6
0	6	2	59.13	58.25	58.12	53.65	66.62	64.95	12.3	15.5	3.2
2	6	2	29.86	29.24	31.36	33.82	39.74	42.10	175.2	172.5	2.7
4	6	2	22.19	21.42	21.51	21.45	27.57	26.14	16.8	4.0	12.8
1	7	2	17.32	17.41	16.84	17.94	19.65	20.39	0.7	-47.5	48.2
3	7	2	14.62	15.19	10.42	17.93	14.64	22.25	125.4	118.0	7.4
5	7	2	25.15	24.25	25.69	25.92	32.37	33.49	3.9	-1.0	4.9
1	9	2	11.03	12.82	11.78	11.69	13.69	15.26	178.9	141.0	37.9
1	0	3	13.19	13.12	11.37	16.38	13.03	19.27	-72.1	-72.0	0.1
3	0	3	45.80	41.63	56.88	58.59	67.24	67.42	179.6	160.0	19.6
5	0	3	24.67	22.42	24.68	31.97	34.43	39.60	-16.6	-15.0	1.6
0	1	3	21.50	21.71	23.13	26.96	30.01	32.38	-11.5	-23.5	12.0
2	1	3	34.75	32.72	43.05	40.93	49.08	47.10	-166.6	165.5	27.9
3	2	3	30.52	28.56	32.85	33.21	39.39	38.15	-2.2	-22.0	19.8
5	2	3	14.46	13.35	15.30	13.98	20.14	18.80	-174.3	-171.0	3.3
0	3	3	33.33	33.71	39.34	42.21	48.73	51.74	168.8	168.5	0.3
2	3	3	43.48	40.93	53.62	51.68	63.09	61.47	-1.5	-8.5	7.0
1	4	3	8.22	7.97	8.96	5.57	7.26	7.43	-10.2	-80.5	70.3
3	4	3	28.80	27.30	31.00	28.56	37.97	35.31	11.1	6.0	5.1
5	4	3	11.41	10.28	12.24	9.87	18.12	16.41	-169.4	-151.0	18.4
0	5	3	23.49	23.31	22.31	23.92	28.18	29.02	-13.2	-28.5	15.3
2	5	3	18.43	17.92	17.95	17.40	22.89	21.26	-168.0	-168.5	0.5
3	6	3	30.97	29.56	33.36	31.80	41.81	40.88	-174.2	-178.5	4.3
0	7	3	9.35	9.23	12.13	11.52	16.84	14.77	11.9	20.5	8.6
2	7	3	28.70	28.01	30.35	28.20	37.84	35.90	-164.6	-173.5	8.9
0	0	4	40.21	40.06	52.09	51.23	62.77	63.07	3.3	12.0	15.3
2	0	4	19.94	19.34	24.23	22.63	31.57	30.49	-173.9	-176.5	2.6
1	1	4	8.50	8.76	10.45	9.18	10.91	11.66	-6.8	-33.0	26.2
0	2	4	14.78	15.54	13.66	19.17	18.37	23.04	147.1	130.5	16.6
4	2	4	12.79	12.20	12.17	14.01	15.53	15.65	171.6	127.0	44.6
1	3	4	20.76	20.87	20.63	21.66	25.84	26.31	174.5	147.0	27.5
3	3	4	11.27	10.54	14.89	10.62	20.57	17.73	19.9	31.0	11.1
0	4	4	30.07	30.28	34.07	34.01	23.54	28.40	176.5	13.5	163.0
2	4	4	9.29	8.90	10.80	9.60	14.56	15.29	6.6	8.0	1.4
0	6	4	32.76	32.36	38.53	37.23	48.39	46.81	5.5	-2.0	7.5

secting points among circles will scatter according to the Gaussian distribution around a true point, if the errors are random. The true phase can then be estimated accurately by the use of probability, as used in the isomorphous-replacement method.

In the present work, the phase angles of the reflexions have been determined by anomalous scattering by the use of white X-rays from an ordinary sealed-off tube. If use is made of the high-intensity 1A X-ray laboratory source, then the time required will be reduced by a factor of about 35, and this method becomes more feasible.

The present method has another demerit: the energy resolution varies together with the diffraction angle, and in a lower Bragg angle region, the resolution reaches a few hundred eV under ordinary conditions. Therefore, it is impossible to make the best use of the anomalous-scattering terms, f' and f'', which vary rapidly in the range of a few electron volts. This demerit can be overcome to some extent if the distance between the incident slit and the sample is varied with the Bragg angle. In this case, it is necessary to make measurements redundantly so that the scaling may be made uniform between neighbouring zones.

The synchrotron radiation is much more effective for the phase determination by the anomalous-scattering effect, because it is a tunable source with high intensity in a wide and continuous energy range. At the present stage, at least, when the synchrotron source is not easy to access for many potential users, the SSD diffractometer may have some merits for use in typical laboratories. The trial experiments reported here may contribute to the future of white X-ray crystallography, even after the intensive sources become more popular.

In the present work, the E_2 and E_3 values used correspond to the region where $|f'(E_2) - f'(E_3)| \simeq 2$, only because the energy resolution is not good enough to use the region where $|f'|$ is very large. However, the value can be made as large as 7 near the K edge if the energy resolution is high, and moreover this value becomes about 25 in the L_{III} edge, as was shown by the

work with a synchrotron source (Phillips, Templeton, Templeton & Hodgson, 1978). In the case of utilizing the L edge, the size of the protein which can be solved by the use of anomalous scattering is considered, as follows. The errors in intensity measurement are usually about 5% at the present time. Let us assume that the intensity change should be 4 times as large as the standard error of the intensity measurements in order to utilize the anomalous scattering effectively. Then, it is necessary to give an intensity change of about 20%. Crick & Magdoff (1956) derived the formula in the case of the isomorphous-replacement method. If this formula can be used, the anomalous scattering is effective for solving a protein structure with a molecular weight of about 20 000. However, it has recently become easier to solve a structure of such a size, if isomorphous replacement is applicable. Therefore, the anomalous scattering is helpful in solving the structures of molecules which are somewhat complicated, but not so complicated as proteins, and do not have any isomorphous derivative.

The authors are indebted to Professor Takéuchi of the University of Tokyo for supplying them with a thin sample of hemimorphite, suitably prepared. The present work has been partly supported by a Grant-in-Aid for Scientific Research (Project No. 140001) from the Ministry of Education.

References

ARTEMYEV, A. N., KABANNIK, V. A., KAZAKOV, Y. N., KULIPANOV, G. N., MELESHKO, E. A., SKLYAREVSKIY, V. V., SKRINSKY, A. N., STEPANOV, E. P., KHLESTOV, V. B. & CHECHIN, A. I. (1978). *Nucl. Instrum. Methods*, **152**, 235–241.

BARCLAY, G. A. & COX, E. G. (1960). *Z. Kristallogr.* **113**, 23–29.

BARTUNIK, H. D. (1978). *Acta Cryst.* A**34**, 747–750.

BLOW, D. M. & CRICK, F. H. C. (1959). *Acta Cryst.* **12**, 794–802.

BONSE, U. & MATERLIK, G. (1976). *Z. Phys.* B**24**, 189–191.

BURAS, B., NIIMURA, N. & OLSEN, J. S. (1978). *J. Appl. Cryst.* **11**, 137–140.

COHEN, R. L., MILLER, G. L. & WEST, K. W. (1978). *Phys. Rev. Lett.* **41**, 381–384.

COLE, H. & STEMPLE, N. R. (1962). *J. Appl. Phys.* **33**, 2227–2233.

CRICK, F. H. C. & MAGDOFF, B. S. (1956). *Acta Cryst.* **9**, 901–908.

CROMER, D. T. (1965). *Acta Cryst.* **18**, 17–23.

DALE, D. & WILLIS, B. T. M. (1966). Report No. R-5195. AERE, Harwell, Oxon.

FUKAMACHI, T. & HOSOYA, S. (1975). *Acta Cryst.* A**31**, 215–220.

FUKAMACHI, T., HOSOYA, S., KAWAMURA, T. & HASTINGS, J. (1977). *J. Appl. Cryst.* **10**, 321–324.

FUKAMACHI, T., HOSOYA, S., KAWAMURA, T., HUNTER, S. & NAKANO, Y. (1978). *Jpn. J. Appl. Phys.* **17** (Suppl. 17-2), 326–328.

FUKAMACHI, T., HOSOYA, S., KAWAMURA, T. & OKUNUKI, M. (1977). *Acta Cryst.* A**33**, 54–58.

FUKAMACHI, T., HOSOYA, S., KAWAMURA, T. & OKUNUKI, M. (1979). *Acta Cryst.* A**35**, 828–831.

FUKAMACHI, T., HOSOYA, S. & OKUNUKI, M. (1976*a*). *Acta Cryst.* A**32**, 104–109.

FUKAMACHI, T., HOSOYA, S. & OKUNUKI, M. (1976*b*). *Acta Cryst.* A**32**, 245–249.

FUKAMACHI, T., HOSOYA, S. & TERASAKI, O. (1973). *J. Appl. Cryst.* **6**, 117–122.

GOLDAK, G. R. (1969). *Acta Cryst.* A**25**, 367–369.

GOLDAK, G. R. (1971). *Acta Cryst.* A**27**, 211–216.

GOLDAK, G. R. (1974). *Acta Cryst.* A**30**, 153–160.

GRENVILLE-WELLS, H. T. & LONSDALE, K. (1954). *Nature (London)*, **173**, 1145–1146.

HERZENBERG, A. & LAU, H. S. M. (1967). *Acta Cryst.* **22**, 24–28.

HILL, R. J., GIBBS, G. V., CRAIG, J. R., ROSS, F. K. & WILLIAMS, J. M. (1977). *Z. Kristallogr.* **146**, 241–259.

HODGSON, K. O., PHILLIPS, J. C. & WLODAWER, A. (1976). *Trans. Am. Crystallogr. Assoc.* **12**, 1–9.

HOLLOWAY, H. (1969). *J. Appl. Phys.* **40**, 2187–2190.

HOPPE, W. & JAKUBOWSKI, U. (1975). *Anomalous Scattering*, edited by S. RAMASESHAN & S. C. ABRAHAMS, pp. 437–461. Copenhagen: Munksgaard.

HOSOYA, S. (1975). *Anomalous Scattering*, edited by S. RAMASESHAN & S. C. ABRAHAMS, pp. 275–287. Copenhagen: Munksgaard.

HOSOYA, S. & FUKAMACHI, T. (1973). *J. Appl. Cryst.* **6**, 396–399.

ITO, T. & WEST, J. (1932). *Z. Kristallogr.* **83**, 1–8.

KAGAN, Y., AFANAS'EV, A. M. & KOHN, V. G. (1979). *J. Phys. C*, **12**, 615–631.

KOETZLE, T. F. & HAMILTON, W. C. (1975). *Anomalous Scattering*, edited by S. RAMASESHAN & S. C. ABRAHAMS, pp. 489–502. Copenhagen: Munksgaard.

MCDONALD, W. S. & CRUICKSHANK, D. W. J. (1967). *Z. Kristallogr.* **124**, 180–191.

MÖSSBAUER, R. L. (1973). *Naturwissenschaften*, **60**, 439–500.

MÖSSBAUER, R. L. (1975). *Anomalous Scattering*, edited by S. RAMASESHAN & S. C. ABRAHAMS, pp. 463–483. Copenhagen: Munksgaard.

PARRATT, L. G. & HEMPSTEAD, C. F. (1954). *Phys. Rev.* **94**, 1593–1600.

PHILLIPS, J. C., TEMPLETON, D. H., TEMPLETON, L. K. & HODGSON, K. O. (1978). *Science*, **201**, 257–259.

PHILLIPS, J. C., WLODAWER, A., GOODFELLOW, J. M., WATENPAUGH, K. D., SIEKER, L. C., JENSEN, L. H. & HODGSON, K. O. (1977). *Acta Cryst.* A**33**, 445–455.

PHILLIPS, J. C., WLODAWER, A., YEVITZ, M. M. & HODGSON, K. O. (1976). *Proc. Natl Acad. Sci. USA*, **73**, 128–132.

SIKKA, S. K. (1969). *Acta Cryst.* A**25**, 396.

SIKKA, S. K. & RAJAGOPAL, H. (1975). *Anomalous Scattering*, edited by S. RAMASESHAN & S. C. ABRAHAMS, pp. 503–514. Copenhagen: Munksgaard.

STAUN OLSEN, J., BURAS, B., JENSEN, T., ALSTRUP, O., GERWARD, L. & SELSMARK, B. (1978). *Acta Cryst.* A**34**, 84–87.

TAKÉUCHI, Y., SASAKI, S., JOSWIG, W. & FUESS, H. (1978). *Proc. Jpn Acad. Ser. B*, **54**, 577–582.

TOKONAMI, M. & HOSOYA, S. (1965). *Acta Cryst.* **18**, 908–916.